AD-A082 102 MASSACHUSETTS INST OF TECH CAMBRIDGE EXPERIMENTAL AS--ETC F/G 17/7
ERROR ANALYSIS OF A DUAL-RANGE NAVIGATION FIX AND DETERMINATION--ETC(U)
OCT 67 G ZACHARIAS N62306-67-C-0122
UNCLASSIFIED RN-31 NL

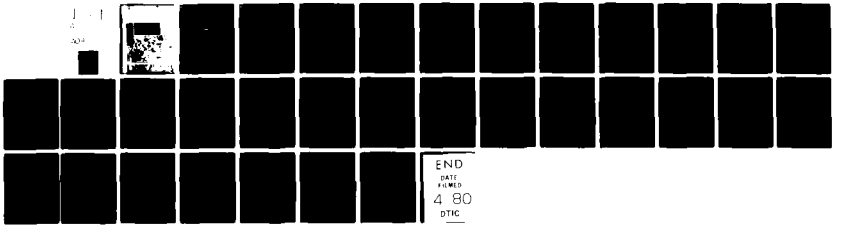

END
DATE FILMED
4 80
DTIC

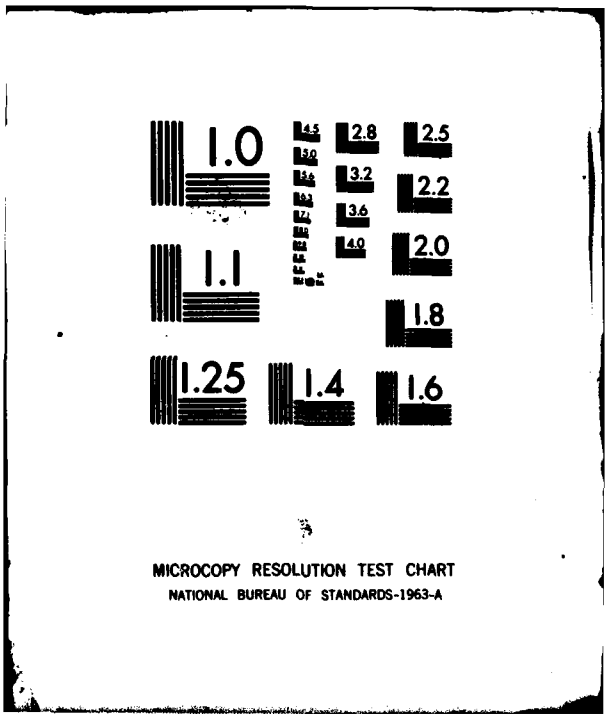
1.0
1.1
1.25
1.4
1.6
1.8
2.0
2.2
2.5
2.8
3.2
3.6
4.0
4.5
5.0
5.6
6.3
7.1
8.0
MICROCOPY RESOLUTION TEST CHART
NATIONAL BUREAU OF STANDARDS-1963-A

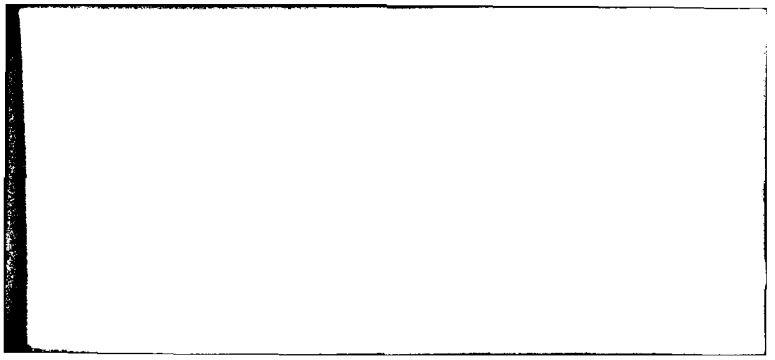

MASSACHUSETTS INSTITUTE OF TECHNOLOGY
DEPARTMENT OF AERONAUTICS AND ASTRONAUTICS
EXPERIMENTAL ASTRONOMY LABORATORY
CAMBRIDGE, MASSACHUSETTS 02139

(14) RN-31

(6) ERROR ANALYSIS OF A DUAL-RANGE NAVIGATION FIX AND DETERMINATION OF AN OPTIMAL SURVEY PATTERN

by

(10) Greg Zacharias

(11) Oct [redacted] 67

(12) 33

Contract N62306-67-C-0122

(15)

887140

MIT

EXPLANATORY NOTE

This is one of a series of Engineering Reports that document the back-ground studies to be used in a system design for HYSURCH (Hydrographic Surveying and Charting System). In general, these reports cover more detail than that finally necessary for a system design, Any subsystem recommendations contained in these reports are to be considered tentative. The reports in this series are.:

RN-22 Soundboat Navigation Equipment and Strategy for HYSURCH by John Hovorka

RN-23 The Role of the HYSURCH Survey Ship in the Production of Nautical Charts by Edwin A. Olsson

RN-24 An Investigation of Side-Looking Radar and Laser Fathometers as HYSURCH Sensors by Jack H. Arabian

RN-25 A Computation Center for Compilation, Revision and Presentation of Hydrographic Chart Materials by Edwin A. Olsson

RN-27 Parameters for the Evaluation of Sonar Depth Measurement Systems by Joel B. Searcy

RN-28 Tidal Measurement, Analysis, and Prediction by J. Thomas Egan and Harold L. Jones

RN-29 Applications of Aerial Photography for HYSURCH by A.C. Conrod

RN-30 Sounding Equipment Studies, by Leonard S. Wilk

RN-31 Error Analysis of a Dual-Range Navigation Fix and Determination of an Optimal Survey Pattern by Greg Zacharias

RN-32 Tethered Balloons for Sounding Craft Navigation Aids by Lou C. Lothrop

These reports were prepared under DSR Contract 70320, sponsored by the U.S. Naval Oceanographic Office Contract Number N62306-67-C-0122. The reports are meant to fulfill the reporting requirement on Sub-system selection as specified in the MIT proposal submitted in response to the Oceanographic Office Request for Quotation, N62306-67-R-005.

ABSTRACT

Off-track navigation errors are analyzed for a vehicle using a dual-range navigation system. A unique survey pattern which minimizes off-track error is found, and this pattern is compared with more conventional tracking patterns. It is suggested that HYSURCH use the standard procedure of circle-riding, with modifications from the local topography.

ERROR ANALYSIS OF A DUAL-RANGE NAVIGATION FIX AND DETERMINATION OF AN OPTIMAL SURVEY PATTERN

This report considers the problem of minimizing tracking errors in a trilateration radio-navigation system*. Errors due to local anomalies (e.g., ground conductivity), are not discussed, since no previous knowledge of the operating area is assumed. The errors which are of interest, however, are those due to the geometry of a range-range fix; hence the conclusions of this study will pertain to any radio-trilateration scheme used in the absence of local disturbances.

There are two types of error to be minimized in designing the HYSURCH navigation system. First, the average error in the soundboat's position must be minimized so as to locate depth soundings with the accuracy required by the overall system specifications. Secondly, the maximum position error must also be minimized in order to allow efficient coverage of the area being surveyed, since any two contiguous areas swept out by a sounding vehicle must overlap by twice the maximum position error, to assure complete coverage. This paper, then, is a study of these errors and their pertinence to the problem of efficient surveying.

The analysis shows that these errors are functions of the soundboat's position and the direction of its track. Hence, minimization of these errors implies a particular track direction for a given position, resulting in a unique minimum-error tracking pattern. Although this pattern(shown in Figure 2) is not to be considered as a practical solution to the error problem, it strongly supports the conventional navigation technique of circle-riding when using a range-range system.

Even with a suggested minimum-error pattern, it is quite apparent that local topography will be a major determining factor of any particular survey strategy. In fact, because of the additional effort involved in matching local characteristics with a general

---

* A similar analysis will be applied to hyperbolic systems if they appear to be appropriate to HYSURCH.

survey strategy, it is quite tempting to totally disregard the minimum-error constraint, in favor of a strategy which is almost wholly determined by the locale. However, this approach implies more time spent on the survey operation, along with a greater number of baselines (i.e., radio beacons) to cover a given area. In addition, it is apparent that the further from shore a survey takes place, the less important will be the local constraints, and thus it will be easier to match the locale with a minimum-error strategy. Consequently, for HYSURCH, it would appear to be well worth the effort spent on determing a minimum-error navigation strategy for a particular locale, since there would result a savings both in the quantity of radio beacons that must be used, and also in the actual survey time.

A particular type of navigation system has been chosen for the error analysis, which uses two range measurements and a baseline in order to determine position, i.e., trilateration. With this position information, the vehicle will attempt to track a predetermined path of large radius of curvature. The vehicle's guidance system will sense the off-path deviation d, and then guide the vehicle so as to null d. However, due to navigation errors, specifically errors in the two ranges, d will be in error. It is this error in d which is the concern of the present analysis.

In Figure 1, the basic navigation triangle is shown. Points A and B represent two known positions, from which the two ranges, ρ_1 and ρ_2, are measured. The distance b between the points A and B is the baseline of the navigation triangle. Assume cartesian coordinates with the origin at A and the abscissa through B. The vehicle's path may then be approximated by a straight line through the point (x_o, y_o) and with slope m.
Similarly, the vehicle's position is the point (x_1, y_1), the intersection of ρ_1 and ρ_2. Hence, the off-path distance d is the perpendicular from (x_1, y_1) to the path. The purpose of the following derivation is to find the error in d due to the errors in ρ_1 and ρ_2.

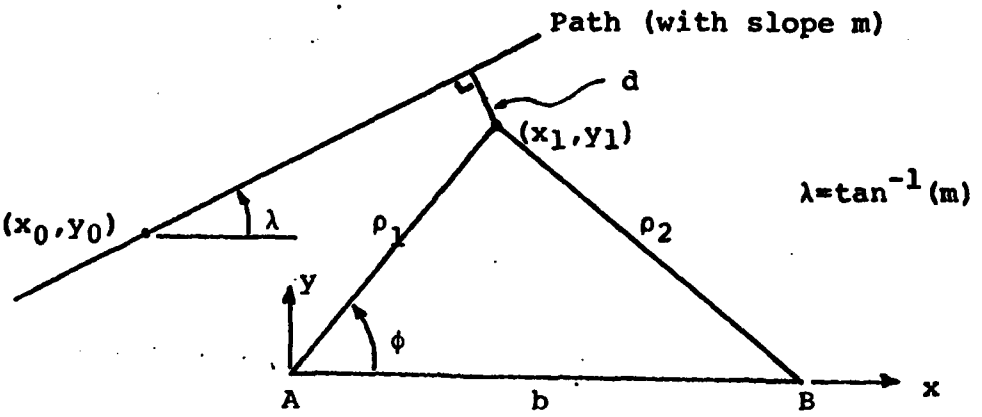

Figure 1: Basic Trilateration Geometry

The distance between point (x_1,y_1) and the path is given by the relationship:

$$d=\frac{1}{\sqrt{m^2+1}}\,|(y_1-y_0)-m(x_1-x_0)|$$

Substituting ρ_1 and ϕ for y_1 and x_1, and ignoring the absolute value sign for the present,

$$d=\frac{1}{\sqrt{m^2+1}}\{\rho_1\sin\phi-y_0-m(\rho_1\cos\phi-x_0)\} \qquad (1)$$

Errors in ρ_1 and ρ_2 ($\delta\rho_1$ and $\delta\rho_2$) result in errors in d and ϕ (δd and $\delta\phi$):

$$d+\delta d=\frac{1}{\sqrt{m^2+1}}\left[(\rho_1+\delta\rho_1)\sin(\phi+\delta\phi)-y_0-m\{(\rho_1+\delta\rho_1)\cos(\phi+\delta\phi)-x_0\}\right]$$

Making small angle approximations, dropping second-order terms, and simplifying,

$$\delta d=\frac{1}{\sqrt{m^2+1}}\{(\rho_1\cos\phi+m\rho_1\sin\phi)\delta\phi+(\sin\phi-m\cos\phi)\delta\rho_1\} \qquad (2)$$

Since $\rho_1^2 + b^2 - 2\rho_1 b\cos\phi = \rho_2^2$, then $\delta\phi = \left[(b\cos\phi - \rho_1)\delta\rho_1 + \rho_2\delta\rho_2\right] / b\rho_1\sin\phi$.

Substituting in eq. 2,

$$\delta d = \frac{1}{b\rho_1\sin\phi\sqrt{m^2+1}}\{\rho_1\delta\rho_1(-\rho_1\cos\phi + b - m\rho_1\sin\phi) + \rho_2\delta\rho_2(\rho_1\cos\phi + m\rho_1\sin\phi)\} \quad (3)$$

Rather than work with ρ_1 and ρ_2 it will be more convenient for later work to shift the co-ordinate system's origin to the bisecting point of the baseline and use an (r,θ) co-ordinate system as shown below.

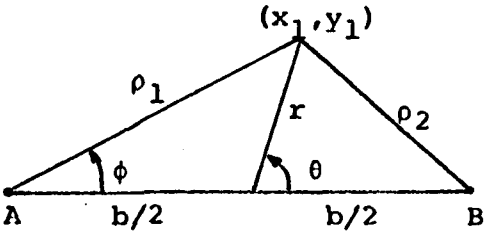

Noting that $\rho_1\sin\phi = r\sin\theta$

$\rho_1\cos\phi = b/2 + r\cos\theta$

and $\rho_1^2 = r^2 + b^2/4 + rb\cos\theta$

$\rho_2^2 = r^2 + b^2/4 - rb\cos\theta$,

squaring eq. 3, and substituting, then

$$(\delta d)^2 = \frac{1}{b^2r^2\sin^2\theta(m^2+1)}\left\{\begin{array}{l}(r^2+b^2/4+rb\cos\theta)(b/2-r\cos\theta-mr\sin\theta)^2(\delta\rho_1)^2 \\ +2\rho_1\rho_2(b/2-r\cos\theta-mr\sin\theta)(b/2+r\cos\theta+mr\sin\theta) \\ (\delta\rho_1)(\delta\rho_2) \quad + (r^2+b^2/4-rb\cos\theta)(b/2+r\cos\theta+mr\sin\theta)^2 \\ (\delta\rho_2)^2\end{array}\right. \quad (4)$$

Assume that the errors in ρ_1 and ρ_2 are uncorrelated, i.e., let $(\delta\rho_1)\ (\delta\rho_2) = 0$. Also, without too great a loss of generality, let $(\delta\rho_1)^2 = (\delta\rho_2)^2 = (\delta\rho)^2$.

Then expanding eq.4 with the above modifications, and simplifying,

$$(\delta d)^2 = \frac{(\delta\rho)^2}{r^2b^2\sin^2\theta(m^2+1)}\left\{\begin{matrix} m^2r^2\sin^2\theta(2r^2+b^2/2)+2mr^2\cos\theta\sin\theta(2r^2-b^2/2) \\ +\frac{r^2b^2}{2}(1-3\cos^2\theta)+b^4/8+2r^4\cos^2\theta \end{matrix}\right\}$$

Letting $R = (r/b)$, $(\delta d)^2$ appears as a function of position (R and θ), slope (m), and range error ($(\delta\rho)^2$):

$$(\delta d)^2 = \frac{(\delta\rho)^2}{R^2\sin^2\theta(m^2+1)}\left\{\begin{matrix} m^2R^2\sin^2\theta(2R^2+1/2)+2mR^2\cos\theta\sin\theta(2R^2-1/2) \\ +(R^2/2)(1-3\cos^2\theta)+1/8+2R^4\cos^2\theta \end{matrix}\right\} \quad (5)$$

This, then, is the error in d which is of interest. The form of the above equation suggest that, in order to minimize $(\delta d)^2$, a particular m should be chosen at a particular position (R,θ). In other words, solving the equation $\frac{\partial(\delta d)^2}{\partial m} = 0$ will result in an equation for m in terms of R and θ. Taking the derivative of eq. 5 and simplifying:

$$\frac{\partial(\delta d)^2}{\partial m} = 0 = \frac{(\delta\rho)^2}{R^2\sin^2\theta(m^2+1)^2}\left\{\begin{matrix} -m^2R^2\cos\theta\sin\theta(4R^2-1) \\ +m\left[4R^4(\sin^2\theta-\cos^2\theta)+2R^2\cos^2\theta-1/4\right] \\ +R^2\cos\theta\sin\theta(4R^2-1) \end{matrix}\right\} \quad (6)$$

If $m \to \infty$, the above expression approaches zero, so that ∞ is one solution for m. Note from equation 5 that

$$\lim_{m\to\infty} (\delta d)^2 = \lim_{m\to\infty} \frac{(\delta\rho)^2}{R^2\sin^2\theta(m^2+1)} \{ m^2R^2\sin^2\theta(2R^2+1/2)\} = (\delta\rho)^2(2R^2+1/2) \tag{7}$$

Hence, with $m = \infty$, $(\delta d)^2 \geq 1/2(\delta\rho)^2$

Now solving for the other two roots of equation 6, let

$$\alpha = R^2(\cos\theta)(\sin\theta)(4R^2-1) \tag{8a}$$

$$\beta = 4R^4(\sin^2\theta-\cos^2\theta)+2R^2\cos^2\theta-1/4 \tag{8b}$$

Then,

$$-\alpha m^2 + \beta m + \alpha = 0, \text{ or}$$

$$m_1 = \frac{-\beta+(\beta^2+4\alpha^2)^{1/2}}{-2\alpha}, \text{ and} \tag{9a}$$

$$m_2 = \frac{-\beta-(\beta^2+4\alpha^2)^{1/2}}{-2\alpha} \tag{9b}$$

Equations 9a and 9b define two values of m, which, when substituted in equation 5, result in two values of $(\delta d)^2$: the minimum and the maximum, respectively, for a given position. To show this analytically is computationally difficult; however, it is shown in the numerical examples to follow that the use of m_1 indeed results in a minimum $(\delta d)^2$.

Figure 2 makes graphic the implications of equation 9a, showing the family of paths that should be followed in order to minimize $(\delta d)^2$. The figure is constructed by computing m_1 at selected positions, and then drawing at each position a short line segment

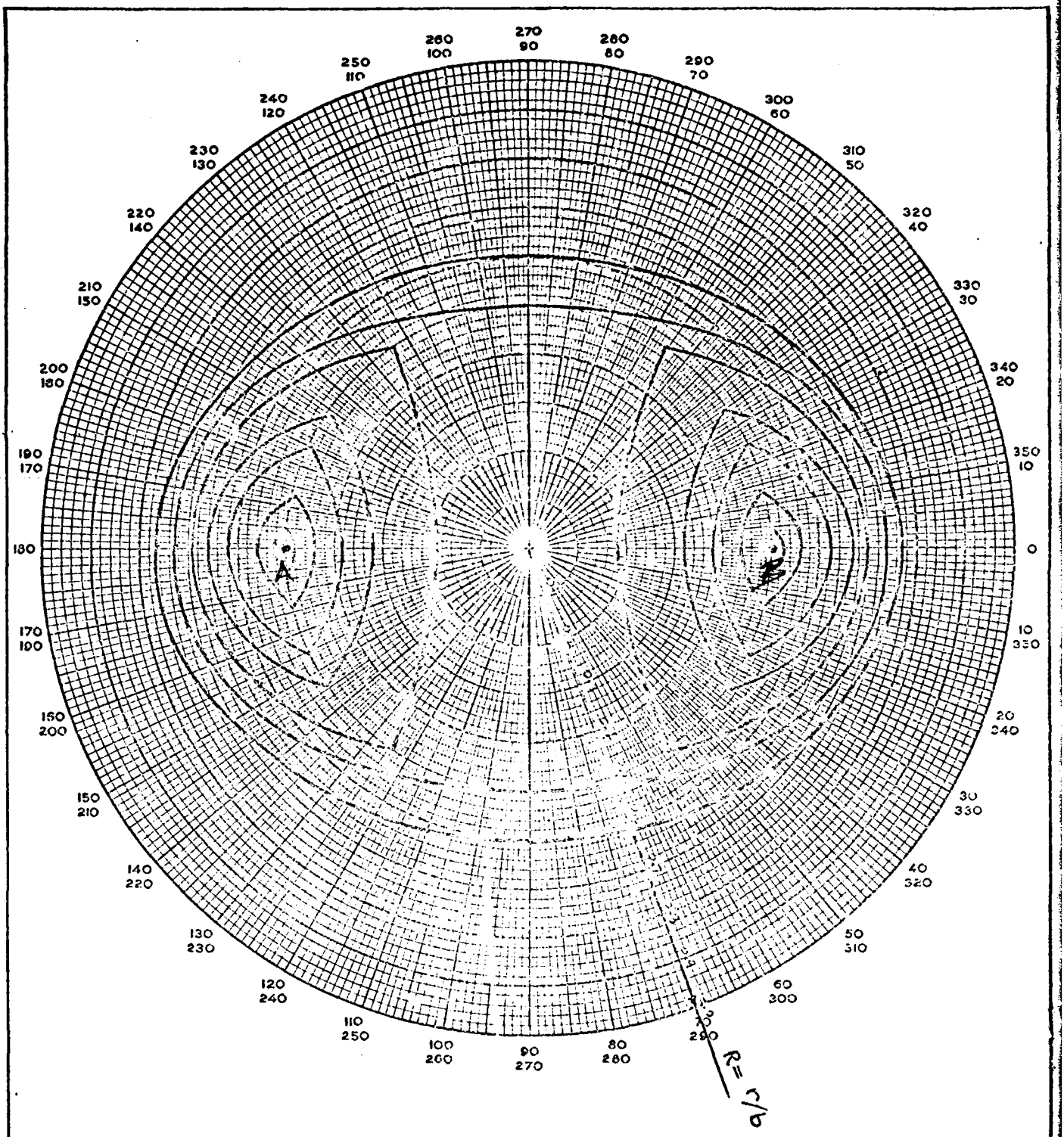

Figure 2: Family of paths for minimum $(\delta d)^2$
(Note that the two dots represent points A and B in figure 1)

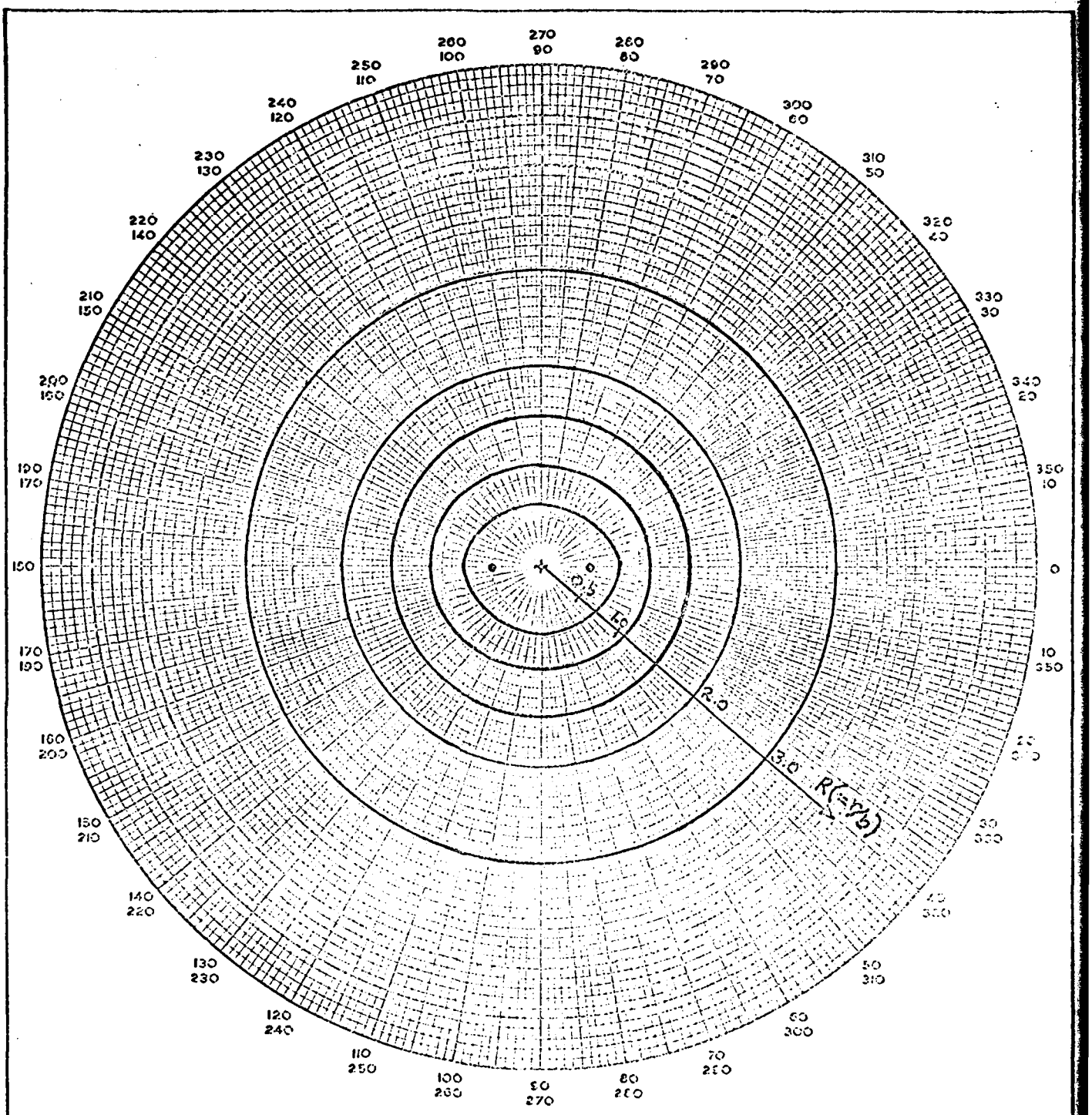

Figure 3: Family of paths for minimum $(\xi_1)^2$

having the computed slope. Smooth curves are then drawn through the line segments in order to aid visualization of the "field" generated by equation 9a. Figure 3 is a larger view of the same field.

Before proceeding further in the analysis, it is of interest to examine some of the characteristics of figures 2 and 3. First, it is quite apparent the patterns are symmetric about the baseline and about its perpendicular bisector. This results simply from the symmetries of equations 8 and 9, in which $m_{1,2}(-\theta) = -m_{1,2}(\theta)$ and $m_{1,2}(\pi-\theta)=-m_{1,2}(\theta)$, where $m_{1,2}$ stands for either m_1 or m_2. Note that this and equation 5 imply that $(\delta d)^2\big|_{\theta} = (\delta d)^2\big|_{-\theta} = (\delta d)^2\big|_{(\pi-\theta)}$.

The behavior of the pattern as $R\to\infty$ is, from figure 3, degeneration into concentric circles. To show this analytically, note that the radical in equation 9 can be expanded by the use of equation 8:

$$\beta^2+4\alpha^2 = \{4R^4(\sin^2\theta-\cos^2\theta)+2R^2\cos^2\theta-1/4\}^2 + 4(4R^2-1)^2R^4\cos^2\theta\sin^2\theta$$

Expanding and simplifying,

$$\beta^2+4\alpha^2 = 16R^8\left[1-\frac{1}{R^2}\cos^2\theta + \frac{1}{8R^4}(4\cos^4\theta-1) - \frac{1}{16R^6}\cos^2\theta + \frac{1}{256R^8}\right]$$

Since $R\to\infty$, it will be sufficient to retain terms of $\frac{1}{R^2}$ or larger. Therefore,

$$\lim_{R\to\infty} (\beta^2+4\alpha^2) = \lim_{R\to\infty} 16R^8\{1-(1/R^2)\cos^2\theta\}, \text{or,}$$

$$\lim_{R\to\infty} (\beta^2+4\alpha^2)^{1/2} = \lim_{R\to\infty} 4R^4\{1-(1/2R^2)\cos^2\theta\}$$

Again letting $m_{1,2}$ represent m_1 or m_2, the above result combined with equation 9 implies

$$\lim_{R\to\infty} m_{1,2} = \lim_{R\to\infty} \frac{2(\cos^2\theta-\sin^2\theta)-(1/R^2)\cos^2\theta \pm \{2-(1/R^2)\cos^2\theta\}}{(1/R^2-4)\cos\theta\sin\theta}$$

Considering m_1 and m_2 separately,

$$\lim_{R\to\infty} m_1 = \lim_{R\to\infty} -\frac{2\cos^2\theta(2-1/R^2)}{\cos\theta\sin\theta(4-1/R^2)} \simeq \lim_{R\to\infty} -\frac{\cos\theta}{\sin\theta}(1-1/4R^2) \qquad (10)$$

$$\lim_{R\to\infty} m_2 = \lim_{R\to\infty} -\frac{4\sin\theta}{\cos\theta(1/R^2-4)} \simeq \lim_{R\to\infty} \frac{\sin\theta}{\cos\theta}(1+1/4R^2) \qquad (11)$$

Since $\lim_{R\to\infty} m_1 = -\cot\theta$, to order $1/R$, and since $m_1 = \tan\lambda$ (from figure 1), then $\lambda = \theta + \pi/2$.

In other words, as $R\to\infty$, the path which generates a minimum $(\delta d)^2$ is always perpendicular to R, and hence, the circularity of the path in figure 3 has been explained. It is of interest to note that, from equations 10 and 11,

$$\left[\lim_{R\to\infty} m_1\right]\left[\lim_{R\to\infty} m_2\right] = \lim_{R\to\infty} -(1-1/16R^4) = -1$$

Hence, as $R\to\infty$ the family of paths generated by m_2 is orthogonal to the family generated by m_1; i.e., maximum-error tracks are perpendicular to minimum-error tracks at large ranges.

Before proceeding with other characteristics of figures 2 and 3, the behavior of $(\delta d)^2$ as $R\to\infty$ is of interest. By substituting into equation 5 the value of m_1 in equation 10 and simplifying ,

$$\lim_{R\to\infty} (\delta d)^2 = \frac{(\delta\rho)^2}{(1-1/2R^2)} \left[\frac{1}{2} + \frac{1}{8R^2} - \frac{\cos^2\theta}{2R^2}\right]$$

Note that to order $1/R$,

$$\lim_{R\to\infty} (\delta d)^2 = \frac{1}{2}(\delta\rho)^2, \text{ using } m_1 \qquad (12)$$

Now, if the same calculation is undertaken, but using m_2 instead of m_1, a strikingly different result is obtained:

$$\lim_{R\to\infty} (\delta d)^2 = \frac{2R^2}{\sin^2\theta} (\delta\rho)^2, \text{ using } m_2 \qquad (13)$$

Comparison of equations 12 and 13 emphasizes the importance of tracking circles centered about the midpoint of the baseline, when maneuvering far from the baseline. This is a strong point to consider in any proposed navigation strategy.

In the region close to the baseline midpoint, a similar investigation of m_1, m_2, and $(\delta d)^2$ may be carried out.

Considering equation 8 and letting R→0,

$$\lim_{R\to o} \alpha = \lim_{R\to o} R^2\cos\theta\sin\theta(4R^2-1) = \lim_{R\to o} -R^2\cos\theta\sin\theta$$

$$\lim_{R\to o} \beta = \lim_{R\to o} \{4R^4(\sin^2\theta-\cos^2\theta)+2R^2\cos^2\theta-1/4\} = \lim_{R\to o} (2R^2\cos^2\theta-1/4)$$

When these values of α and β are substituted into equation 10, letting $m_{1,2}$ again represent m_1 or m_2, a second-order approximation results:

$$\lim_{R\to o} m_{1,2} \simeq \lim_{R\to o} \frac{1-8R^2\cos^2\theta \pm (1-8R^2\cos^2\theta)}{8R^2\cos\theta\sin\theta} \qquad (14)$$

Separating m_1 and m_2,

$$\lim_{R\to o} m_1 = \lim_{R\to o} \frac{1-8R^2\cos^2\theta}{4R^2\cos\theta\sin\theta} = \infty \qquad (15)$$

$$\lim_{R\to o} m_2 = 0 \qquad (16)$$

Equation 15 thus describes that part of figure 2 where R is small. Equation 16 implies orthogonality between the m_1 family of paths and the m_2 family when R is small, as was also true for large R.

As before, the behavior of $(\delta d)^2$, in the region near the base-line midpoint, is of concern here. Since $\lim_{R\to o} m_1 = \infty$, it follows from equation 7 that, to order 1/R,

$$\lim_{R\to o} (\delta d)^2 = \frac{1}{2}(\delta\rho)^2 \quad \text{using } m_1 \qquad (17)$$

As a bsis for comparison, the behavior of $(\delta d)^2$ in this region, using m_2 instead of m_1, again shows sharp contrast with the results obtained by using m_1. If equations 5 and 16 are combined, and only terms of order R^2 are retained, then

$$\lim_{R\to o} (\delta d)^2 = \lim_{R\to o} \frac{(\delta\rho)^2}{R^2\sin^2\theta}\{(R^2/2)(1-3\cos^2\theta)+ 1/8\}$$

Hence, to the same order of approximation as obtained in equation 17,

$$\lim_{R\to o} (\delta d)^2 = \lim_{R\to o} \frac{(\delta\rho)^2}{8R^2\sin^2\theta} \quad \text{using } m_2 \qquad (18)$$

Again, the importance of tracking the m_1 family of paths (in this case where R→o)is apparent.

The final point of discussion of figures 2 and 3 is the rather disconcerting set of discontinuities of R=1/2, shown in figure 2. That this is indeed the situation, can be shown in the following manner.

Let R = (1/2 - ε) where ε→o. Then from equation 8a

$$\lim_{R\to\frac{1}{2}^-} \alpha = \lim_{\varepsilon\to o} (1/2-\varepsilon)^2\cos\theta\sin\theta\{4(1/2-\varepsilon)^2-1\}$$

$$\simeq \lim_{\varepsilon\to o} (1/4-\varepsilon)\cos\theta\sin\theta(-4\varepsilon)$$

Similarly, from equation 9b,

$$\lim_{R\to\frac{1}{2}^-} \beta \simeq \lim_{\varepsilon\to o} -2\varepsilon\sin^2\theta$$

Then, with the above results substituted in equation 9,

$$\lim_{R\to\frac{1}{2}^-} m_{1,2} = \lim_{\varepsilon\to 0} \frac{2\varepsilon\sin^2\theta\pm\{4\varepsilon^2\sin^4\theta+4(16\varepsilon^2)(1/16-(1/2)\varepsilon)\cos^2\theta\sin^2\theta\}^{1/2}}{(-2)(-4\varepsilon)(1/4-\varepsilon)\cos\theta\sin\theta}$$

Simplifying,

$$\lim_{R\to\frac{1}{2}^-} m_{1,2} = \frac{\sin\theta\pm 1}{\cos\theta} \qquad (19)$$

In a similar fashion, it is readily found that

$$\lim_{R\to\frac{1}{2}^+} m_{1,2} = \frac{-\sin\theta\pm 1}{-\cos\theta} \qquad (20)$$

Multiplying equations 19 and 20 together.

$$\left[\lim_{R\to\frac{1}{2}^-} m_{1,2}\right]\left[\lim_{R\to\frac{1}{2}^+} m_{1,2}\right] = \frac{-1}{\cos^2\theta}(-\sin^2\theta\pm\sin\theta\mp\sin\theta+1)=-1 \qquad (21)$$

Hence, not only has it been shown that there is a discontinuity at R = 1/2 (for both the m_1 and m_2 families), but equation 21 shows that this discontinuity is always a right angle. This is obviously an undesirable feature in any navigation pattern, but it is not as restricting as it may appear. To show this, it is only necessary to consider the behavior of $(\delta d)^2$ as R→1/2. If R = 1/2 is used in equation 5, then the result reduces to

$$(\delta d)^2\Big|_{R=1/2} = \frac{(\delta\rho)^2}{\sin^2\theta(m^2+1)}\{(m^2+1)\sin^2\theta\} = (\delta\rho)^2$$

Hence, at R=1/2, $(\delta d)^2$ is totally independent of m. In addition, as will be shown shortly, $(\delta d)^2$ is generally insensitive to m in the region R=1/2.

A fair question to ask, after having discussed figures 2 and 3 in some detail, is: how much departure from the minimum $(\delta d)^2$ patterns is allowed before errors become important? In other words, is it possible to choose $m = m_1+\Delta m$ such that $(\delta d)^2\Big|_{(m_1+\Delta m)}$ is not appreciably greater than $(\delta d)^2\Big|_{m_1}$?

The answer is obviously affirmative at R=1/2 because there $(\delta d)^2 = (\delta\rho)^2$ for all m. However, from the comparison of equations 17 and 18, it would appear that $(\delta d)^2$ is quite sensitive to a change in m for the region R→o. A similar conclusion may be drawn from equations 12 and 13 for the region R→∞ . The quickest check on the regions in between is simply to consider a single position and plot $(\delta d)^2/(\delta\rho)^2$ vs $\lambda(=\tan^{-1}m)$ for this position. This may be repeated

for a number of positions, and the results compared. This has been done in figures 4 through 10. Even from this small sample of points, the following conclusions may be drawn:

1) At R = 1/2, $(\delta d)^2 = (\delta\rho)^2$ and is independent of λ .
2) As R increases from R = 1/2, and as R decreases from R = 1/2 the minimum becomes more and more sharply defined; i.e., it becomes imperative to use a slope very close to m_1, in order to keep $(\delta d)^2$ small.
3) As $\theta \to 0$ and as $\theta \to 180^\circ$, the same effect is seen: a more sharply defined minimum.

A more detailed examination of the above trends can be accomplished by simply drawing more graphs. However, it is more instructive to use a mapping technique of the following form. If an arbitrary value K is chosen for $(\delta d)^2$, such that K is greater than the minimum and less than the maximum, and if $\lambda_1 = \tan^{-1} m_1$, $\Delta\lambda$ may be found, such that $(\delta d)^2\big|_{(\lambda_1+\Delta\lambda)} = K$. To illustrate this, consider figures 7 and 10. If $K = 10\ (\delta\rho)^2$, then for figure 7 (R=1.0 and $\theta=5^\circ$), $\Delta\lambda = \pm 14^\circ$ and for Figure 10 (R=5.0, and $\theta=5^\circ$), $\Delta\lambda = \pm 2^\circ$. Thus, it may be concluded that the minimum is much more sharply defined in Figure 10 than in Figure 7. Hence, $(\delta d)^2$ is more sensitive to m at $(5.0, 5^\circ)$ than at $(1.0, 5^\circ)$, necessitating the use of a slope close to m_1 when working in the region around $(5.0, 5^\circ)$. This approach may be used for all points on the plane, and each point may be associated with a particular $\Delta\lambda$. A typical result is shown in Figure 11.

Here, points having approximately the same $\Delta\lambda$ (i.e., approximately the same sensitivity to λ) are identified by the same symbol. What results, then, is a contour map of the sensitivity of $(\delta d)^2$ to variations in λ about λ_1 (or m about m_1). A blank portion of the map in between two marked portions indicates an intermediate value of $\Delta\lambda$. K was chosen to be $10\ (\delta\rho)^2$; the values of $\Delta\lambda$ are given in the legend. Note that the area in which $\Delta\lambda = \pm 90^\circ$ is a region in which $(\delta d)^2$ is always less than $10\ (\delta\rho)^2$.

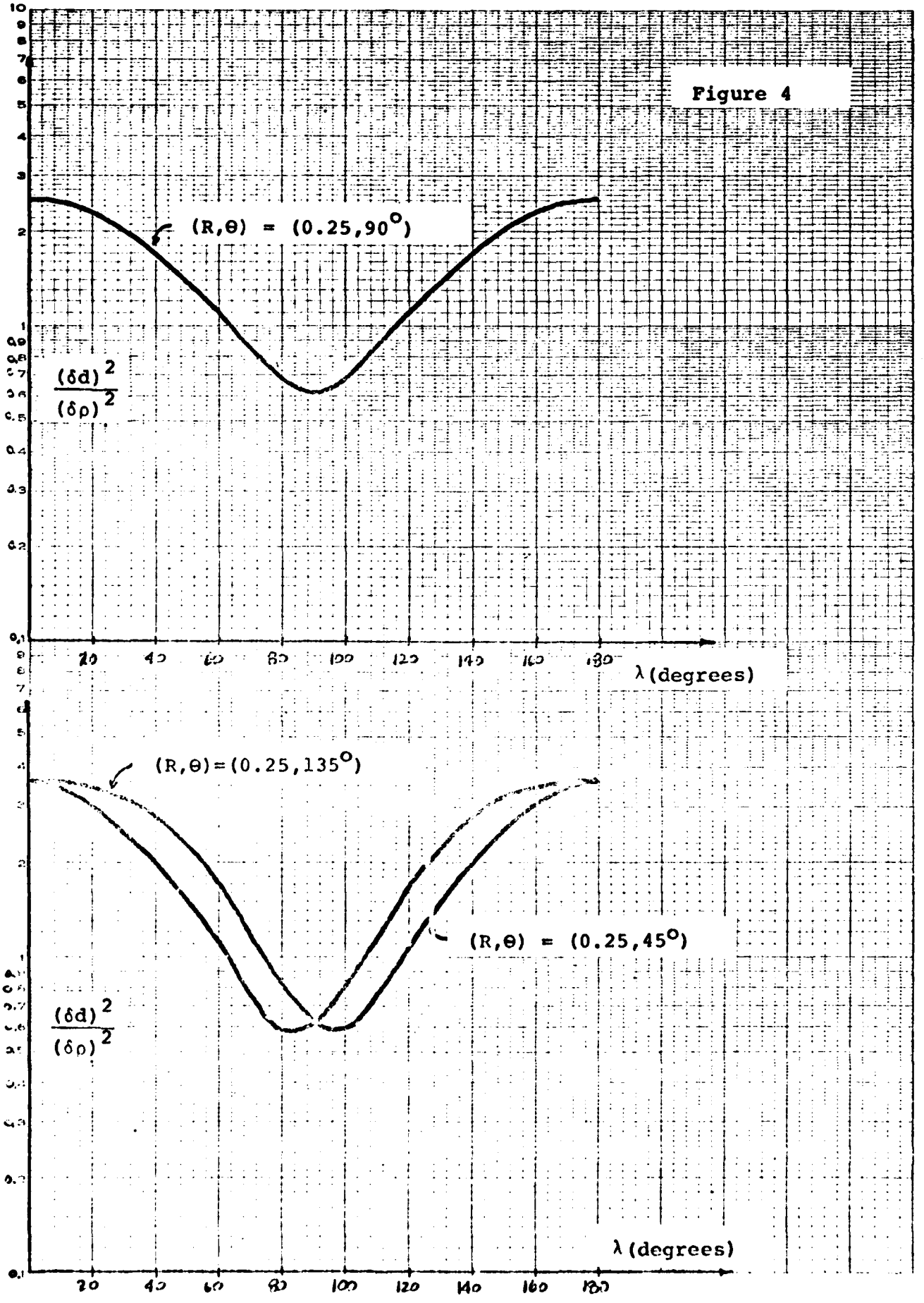
Figure 4
(R,θ) = (0.25,90°)
$\frac{(\delta d)^2}{(\delta \rho)^2}$
λ (degrees)
(R,θ)=(0.25,135°)
(R,θ) = (0.25,45°)
$\frac{(\delta d)^2}{(\delta \rho)^2}$
λ (degrees)

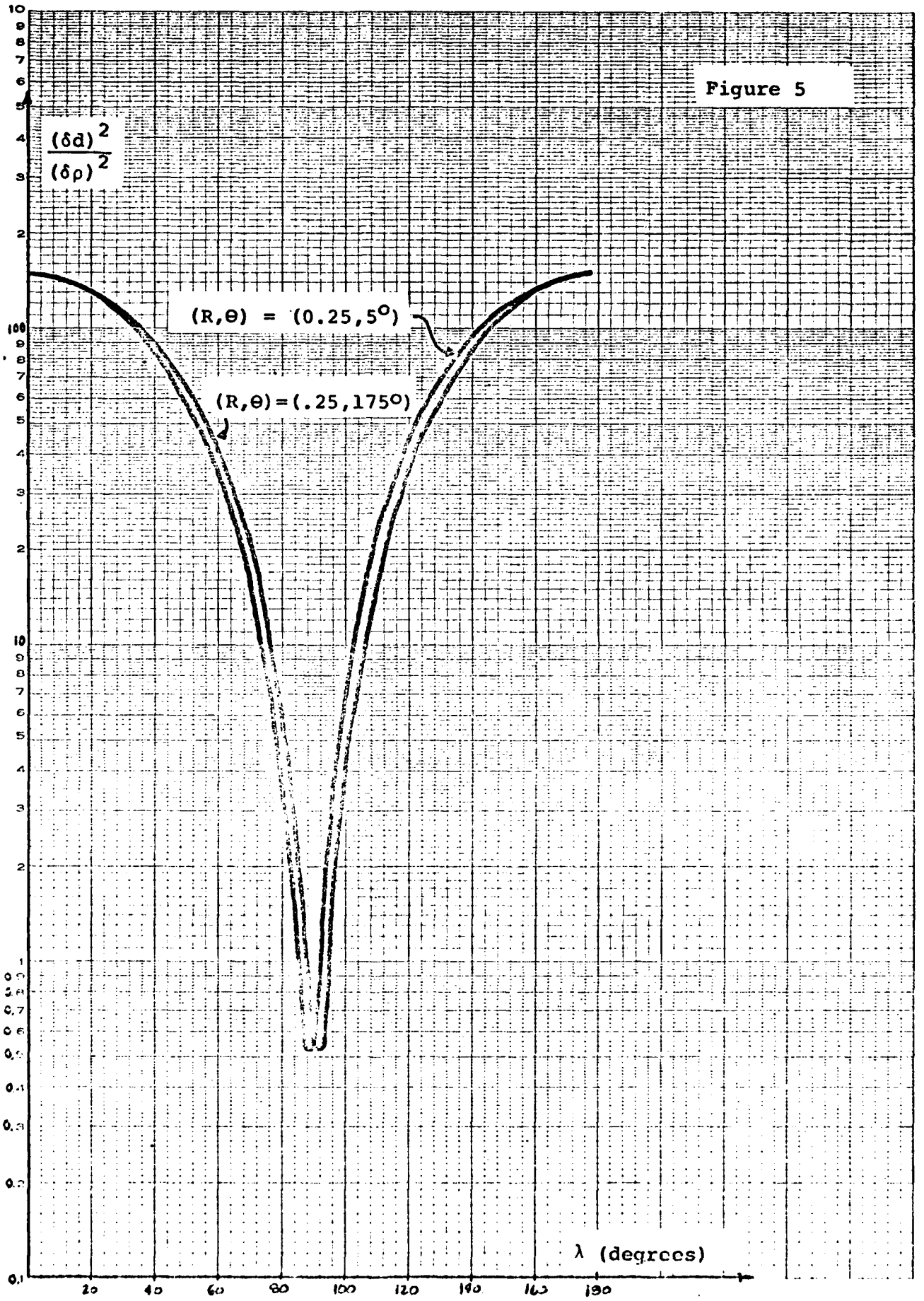
Figure 5
$\frac{(\delta d)^2}{(\delta \rho)^2}$
(R,Θ) = (0.25,5°)
(R,Θ)=(.25,175°)
λ (degrees)
20
40
60
80
100
120
140
160
180
EUGENE DIETZGEN CO.
NO. 340-L410 DIETZGEN GRAPH PAPER
SEMI-LOGARITHMIC
4 CYCLES X 10 DIVISIONS PER INCH

Figure 6

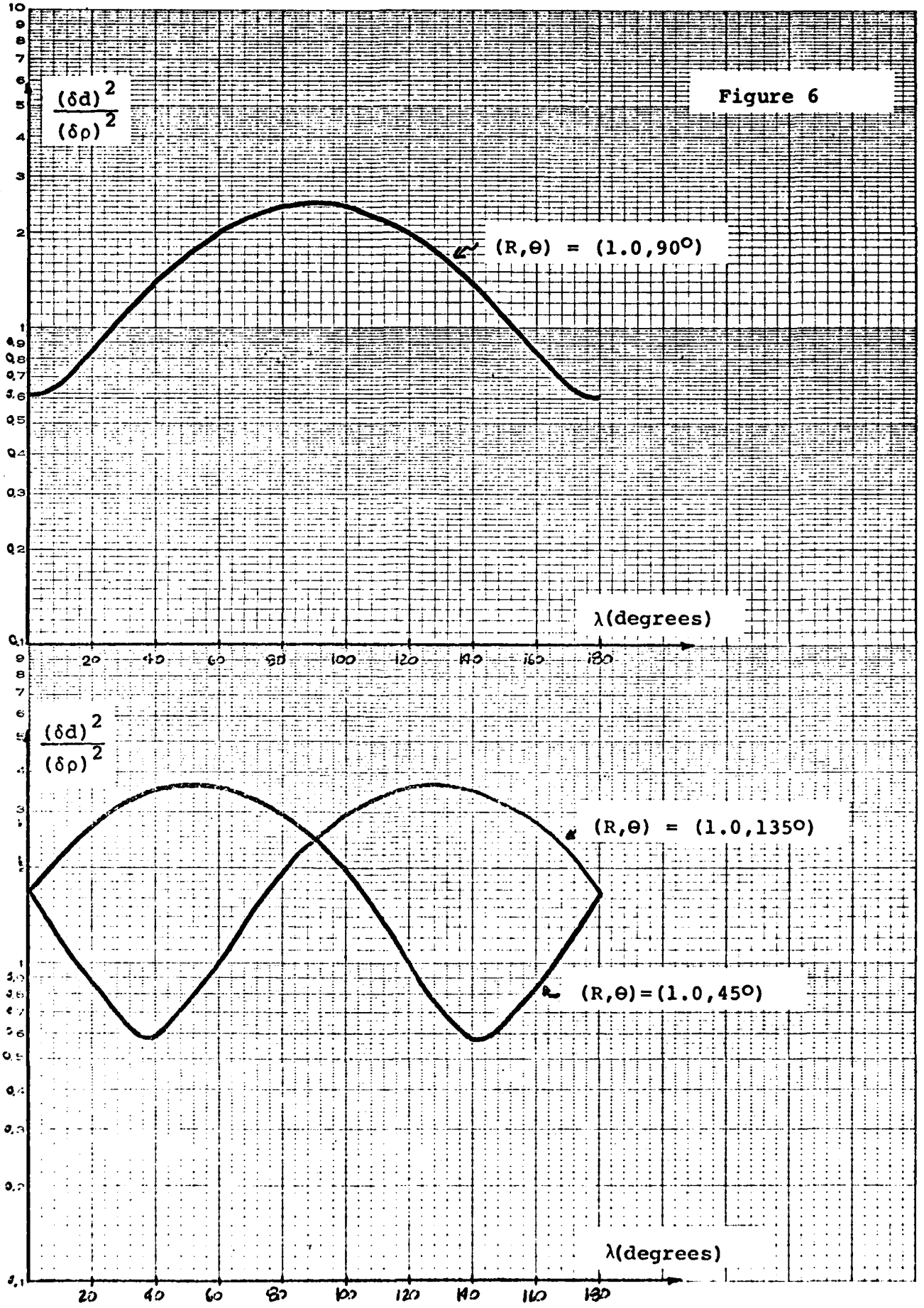

EUGENE DIETZGEN CO.

NO. 340-L410 DIETZGEN GRAPH PAPER
SEMI-LOGARITHMIC
4 CYCLES X 10 DIVISIONS PER INCH

Figure 7

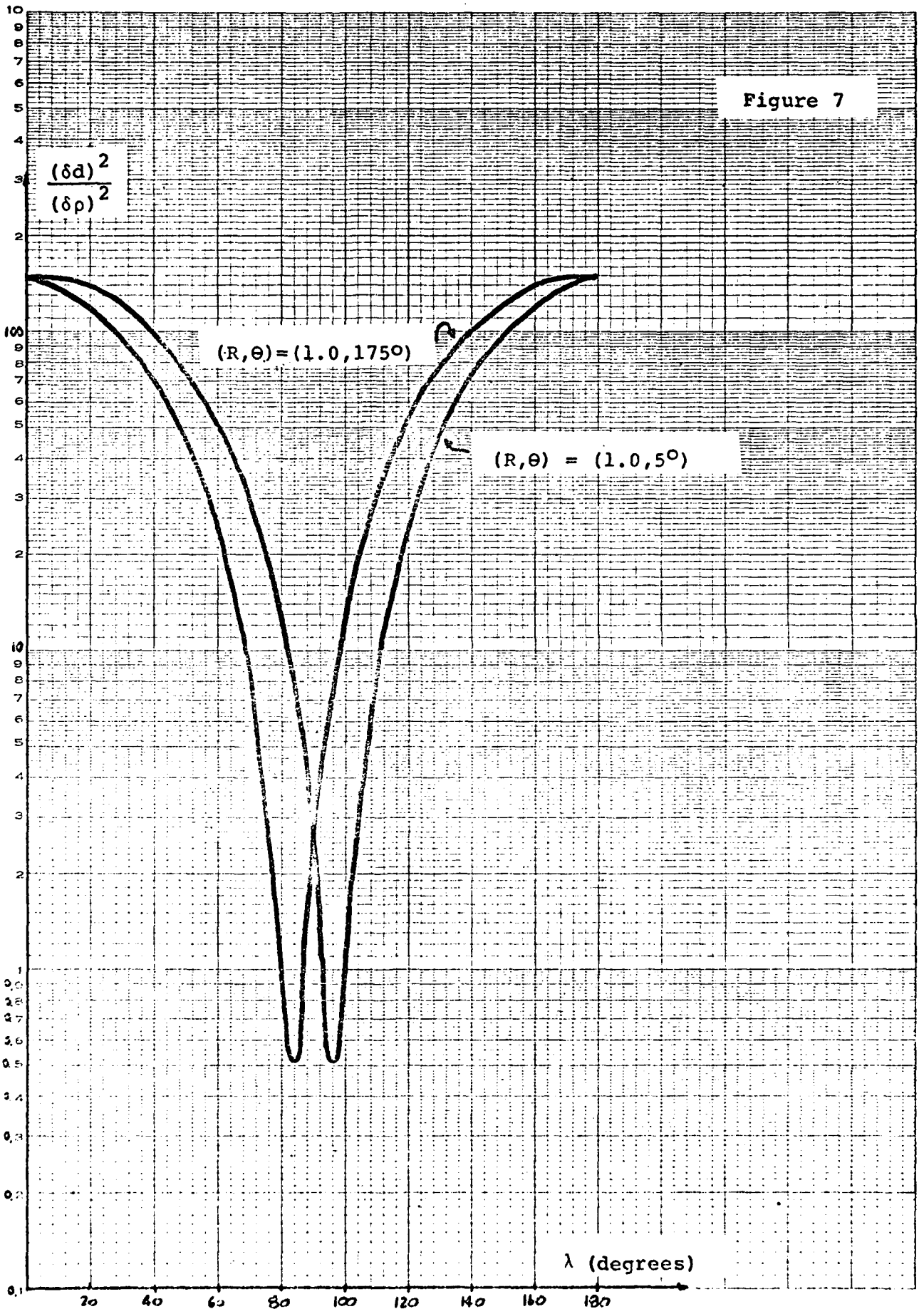

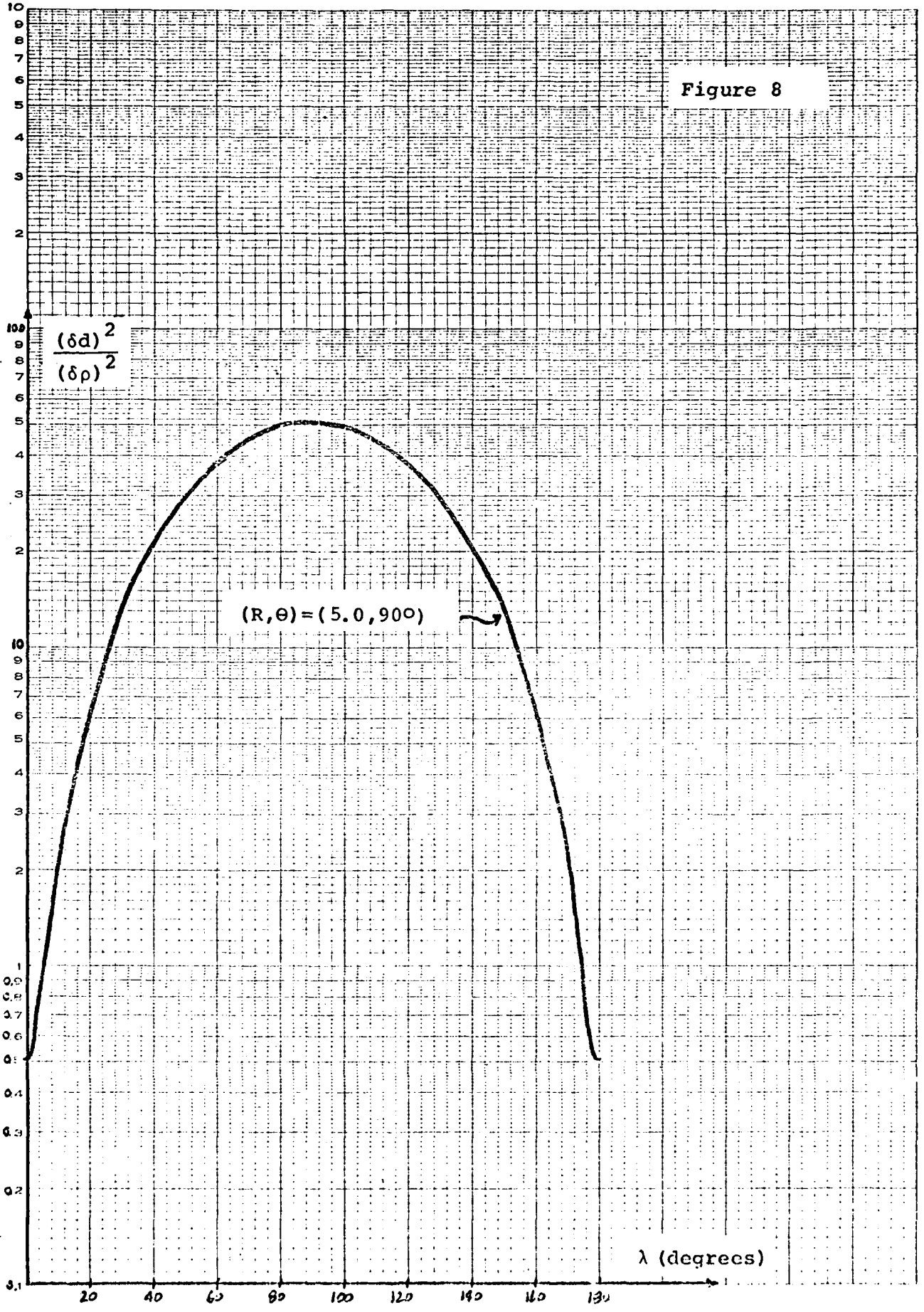
Figure 8
$\frac{(\delta d)^2}{(\delta \rho)^2}$
(R,Θ)=(5.0,90°)
λ (degrees)
20
40
60
80
100
120
140
160
180
EUGENE DIETZGEN CO.
NO. 340-L410 DIETZGEN GRAPH PAPER
SEMI-LOGARITHMIC
4 CYCLES X 10 DIVISIONS PER INCH

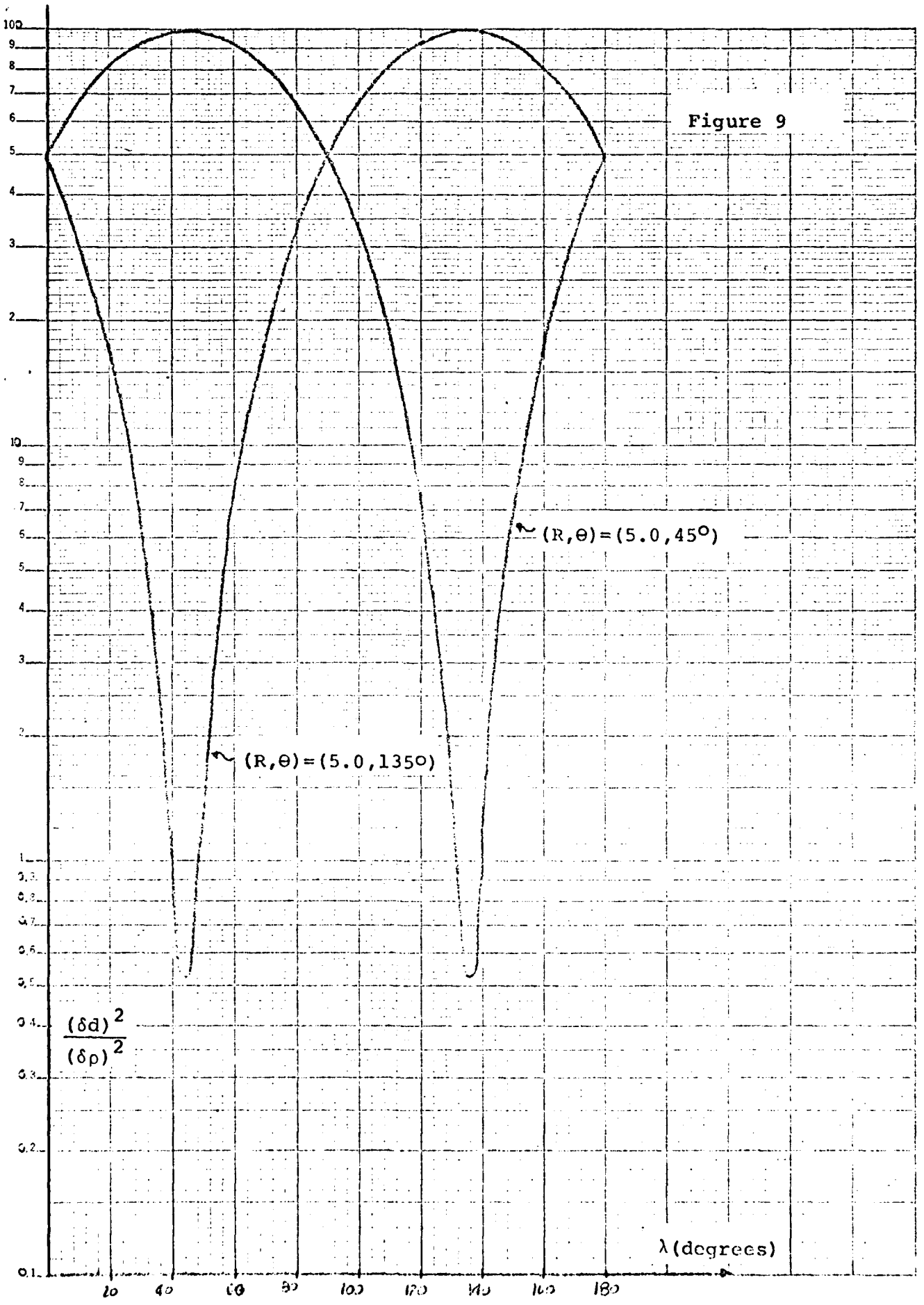
Figure 9
(R,θ)=(5.0,45°)
(R,θ)=(5.0,135°)
$\frac{(\delta d)^2}{(\delta \rho)^2}$
λ(degrees)

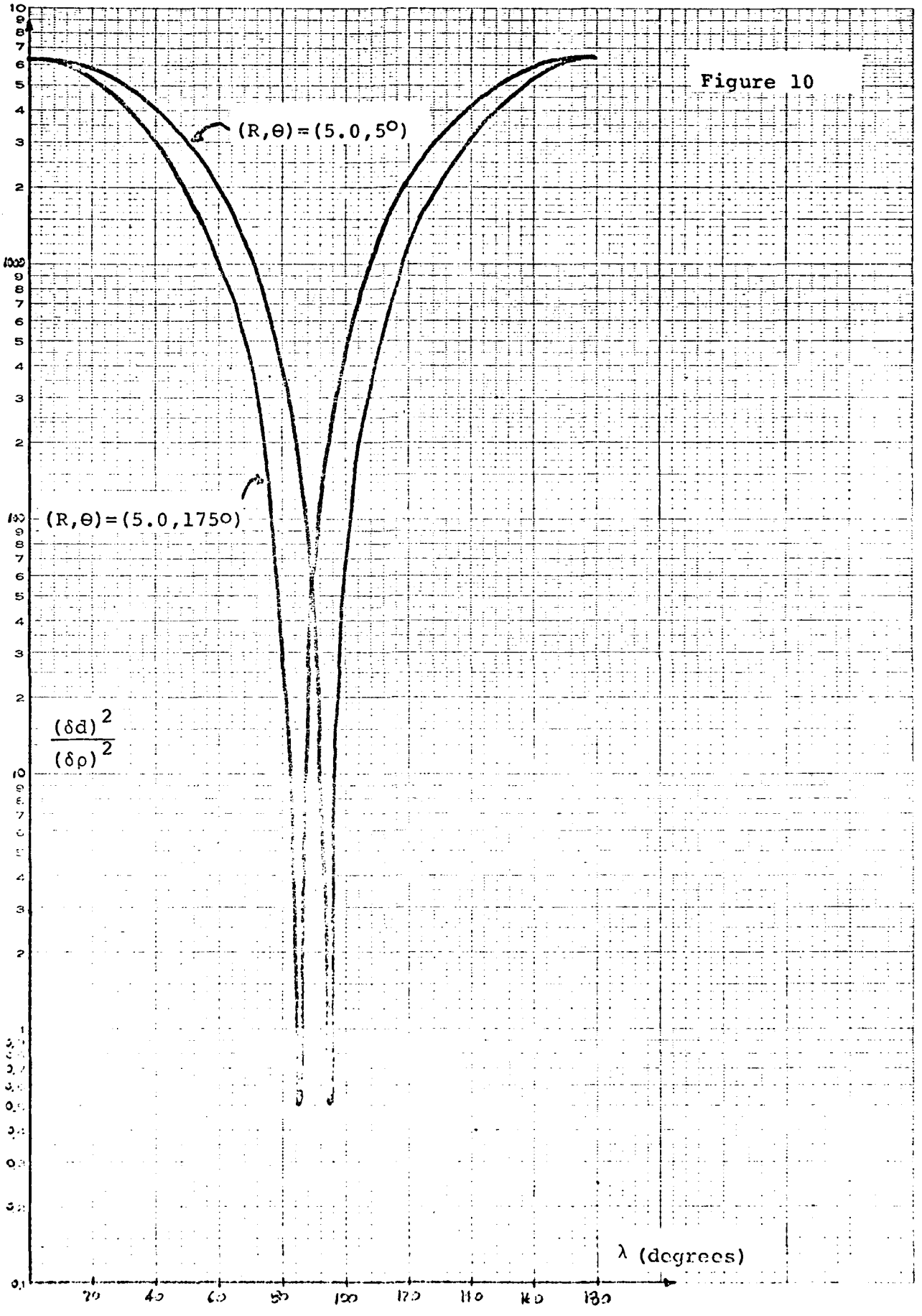

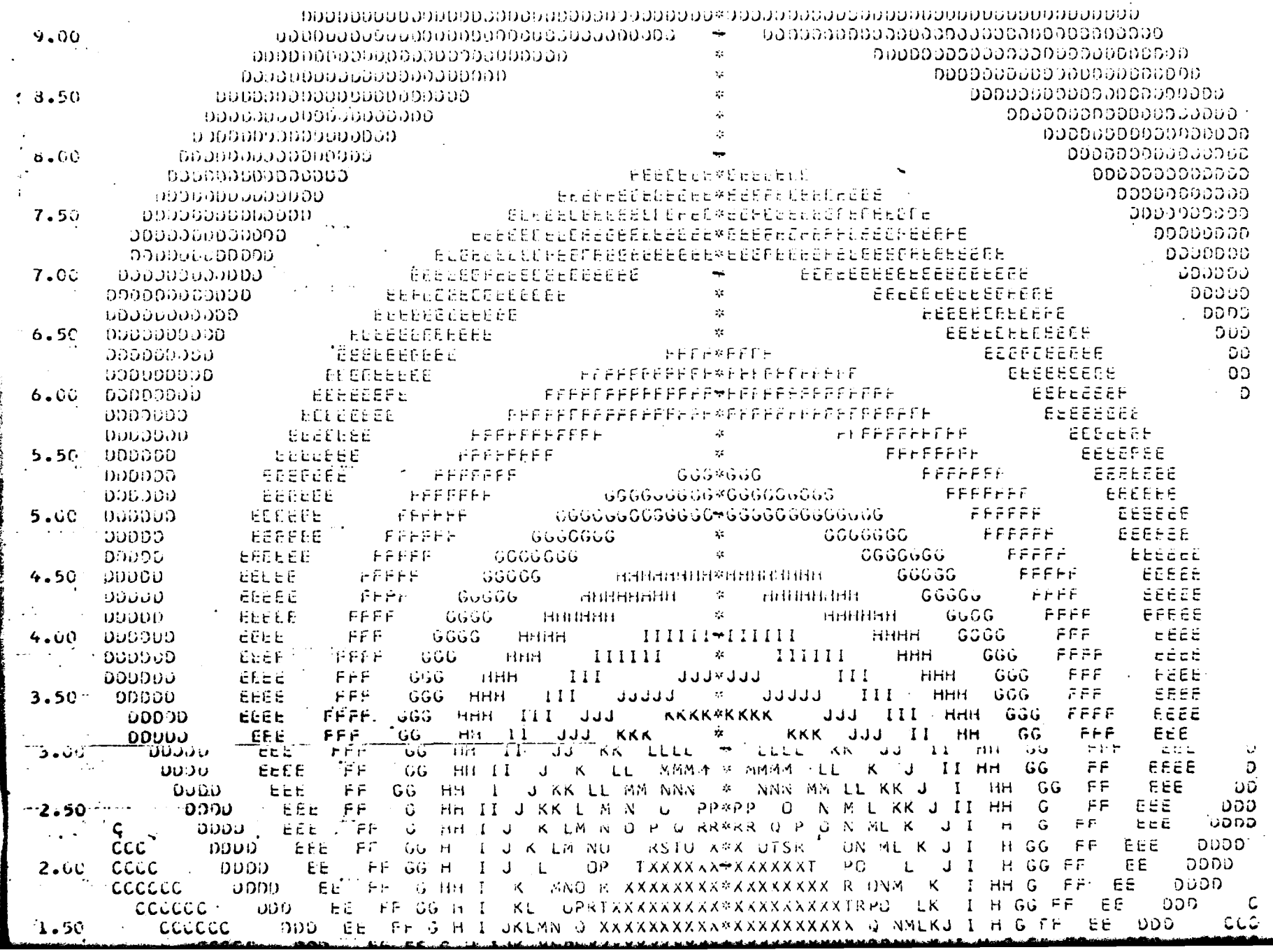
9.00
8.50
8.00
7.50
7.00
6.50
6.00
5.50
5.00
4.50
4.00
3.50
3.00
2.50
2.00
1.50

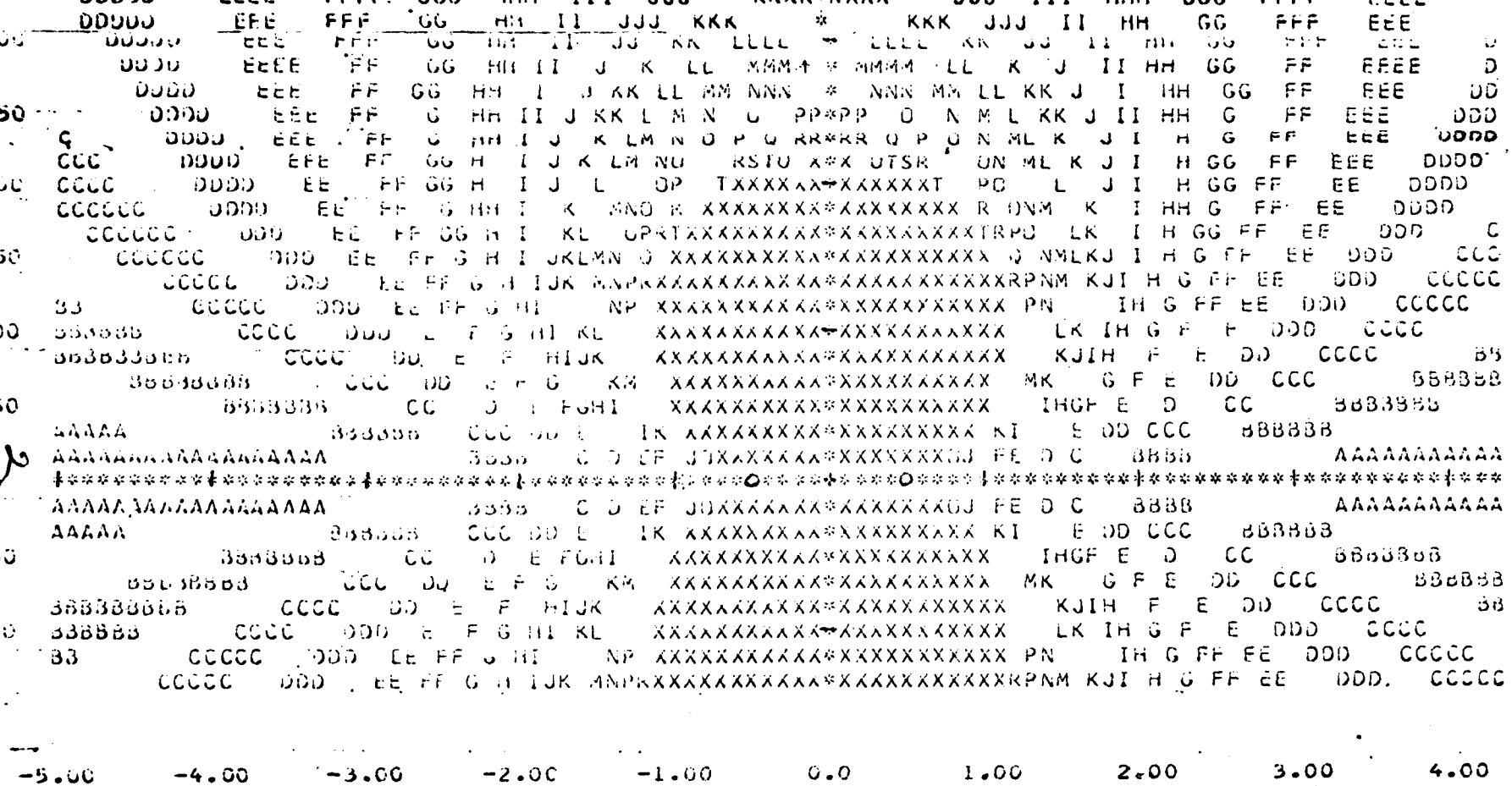

The following is a tabulation of the various regions and their associated values of $\Delta\lambda$ (in degrees):

A	(0 - 2)	G	(24 - 26)	M	(48 - 50)	S	(72 - 74)
B	(4 - 6)	H	(28 - 30)	N	(52 - 54)	T	(76 - 78)
C	(8 - 10)	I	(32 - 34)	O	(56 - 58)	U	(80 - 82)
D	(12 - 14)	J	(36 - 38)	P	(60 - 62)	V	(84 - 86)
E	(16 - 18)	K	(40 - 42)	Q	(64 - 66)	W	(88 - 90)
F	(20 - 22)	L	(44 - 46)	R	(68 - 70)	X	(92 - 94)

Fig. 11: Contour map of $(\delta d)^2$ sensitivity to slope.

Naturally, it is desirable to avoid regions of high sensitivity, and thus figure 11 qualitiatively shows the areas in which accurate navigation is difficult. Once the accuracy requirements are stated, and once the limitations on heading accuracy are known (i.e.$\Delta\lambda$), then, by the use of such a map, definite regions to avoid may be graphically illustrated.

At this point, it is well to recognize that, so far, only one particular navigation pattern has been suggested: that of the family of curves shown in figures 2 and 3. The obvious advantage of this pattern is the genration of a minimum $(\delta d)^2$ for any position (the minimum $(\delta d)^2$ ranging between $0.5(\delta\rho)^2$ and $1.0(\delta\rho)^2$). However, it is also clear that following such a pattern would not be a simple affair, even if curved paths are used to approximate the discontinuities at R=1/2. Perhaps the most useful aspect of this pattern is its use as a standard, with which to compare other patterns. Obviously, all other patterns will yield a distribution of higher valued $(\delta d)^2$, but some may be simpler to track.

One possible pattern is a family of straight lines, oriented at some angle with respect to the baseline. At first, this appears to offer a great deal of simplification compared with the optimal pattern in figures 2 and 3. However, it must be remembered that straight lines are not simple curves when working with a non-cartesian system (such as a range-range system), but usually involve rather complicated formulas. In addition, the maintenance of a constant slope, while navigating along a straight line, implies a rapid fluctuation of $\Delta\lambda$. This results from the fact that the straight line slope is constant , while the slope λ_1, resulting in a minimum $(\delta d)^2$, varies rather markedly with position (as shown in figure 2). Hence,the difference $(\Delta\lambda)$ between the slope used and λ_1, also varies quite a bit. This then results in a large variation of $(\delta d)^2$.

As an example of this problem, consider the situation in which the pattern is a set of straight lines parallel to the baseline

($\lambda = 0^{o}$). Then, from figures 4 and 5, it may be noted that:

at R = .25 $\quad \theta = 45^{o}$, $(\delta d)^2 = 3.6\ (\delta\rho)^2$
and at R = .25 $\quad \theta = 5^{o}$, $(\delta d)^2 = 150\ (\delta\rho)^2$

and so on. This variation is undesirable, and when considered in conjunction with the basic difficulty of following straight lines with a range-range system, it appears that another pattern should be considered.

The pattern which will now be suggested makes use of the basic geometry of the range-range navigation system: a set of concentric circles about one of the two endpoints of the baseline. An immediate advantage of this pattern is that in order to stay on one circle, it is only necessary to keep one of the range readings (ρ_1 or ρ_2) constant. A second advantage is less obvious, but this will be shown in the following evaluation of $(\delta d)^2$ for this pattern.

In the figure below, AB ⊥ BC for a

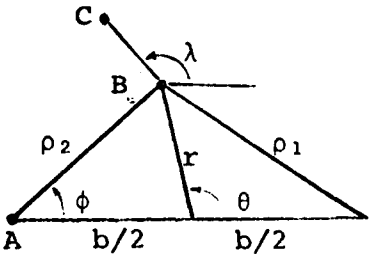

circular path about point A. Hence, $\lambda = \phi + 90^{o}$. Therefore, $m = \tan\lambda = -\cot\phi$

but $\rho_1 \sin\phi = r \sin\theta$

$\rho_1 \cos\phi = b/2 + r\cos\theta$

$$\therefore\ m = -\frac{b/2 + r\cos\theta}{r\sin\theta} = -\frac{1/2 + R\cos\theta}{R\sin\theta} \qquad (R = r/b)$$

Substituting the above result for m in Equation 5 and simplifying,

$$(\delta d)^2 = \frac{(\delta\rho)^2 R^2 \sin^2\theta}{R^2\sin^2\theta(1/4 + R\cos\theta + R^2)} \quad \{ R^2 + 1/4 + R\cos\theta \} = (\delta\rho)^2$$

Thus, this pattern is simple and relatively straight-forward to implement, and results in $(\delta d)^2$ always equalling $(\delta\rho)^2$.

CONCLUSION

The object of this analysis has been to suggest a navigation strategy which minimizes the square of the off-track positon error $\{(\delta d)^2\}$, in order to allow efficient surveying. In order to come to some specific conclusions, a particular means of navigation was chosen: a two range fix with a known baseline, and errors ($\delta\rho$) occuring only in the two range measurements. Naturally, this is an extremely simplified model of a situation in which range-range equipment is used; however, it is a fair approximation, since the greatest errors are expected to come from the range infomration.

Given that the navigating vehicle is nominally tracking a path with a large radius of curvature, it has been shown that one particular family of paths should be tracked in order to minimize $(\delta d)^2$ (figures 2 and 3). Following this pattern results in a maximum $(\delta d)^2$ of 1.0 $(\delta\rho)^2$ and a minimum of 0.5 $(\delta\rho)^2$.

This pattern is not proposed as practical, except as a standard against which to measure other patterns.

Two possible survey patterns have been considered: parallel lines at some angle to the baseline, and circular arcs about either end of the baseline. As was discussed previously, straight lines impose both an undesirable amount of computation, and a large variation of $(\delta d)^2$. Circles, on the other hand, are the simplest possible curves (in range-range co-ordinates), while at the same time resulting in a $(\delta d)^2$ always equalling 1.0 $(\delta\rho)^2$ (a value comparable to the optimal path values). It appears, then, that a family of circular paths is a good first choice for a navigation pattern.

Naturally, other considerations are expected to modify this first choice; an example is the effect of the vehicle's heading accuracy, $\Delta\lambda$, on $(\delta d)^2$. Considering the contour map of $(\delta d)^2$ sensitivity in figure 11, it can be seen, that, given a value for $\Delta\lambda$ and for a maximum allowable $(\delta d)^2$, the "allowable" region for navigation will be a large-waisted figure-eight. Thus, an

additional constraint may be placed on the navigation strategy: that of a specific area within which to navigate.

It is clear that there are yet more constraints to be applied. For example, there are other aspects of the navigation problem, such as determining position, which must be considered Also, the guidance and control interface must be kept in mind so as to allow a workable navigation strategy. Finally, the physical characteristics of the area being surveyed , such as the coastline shape, must modify the general strategy in order to accomplish an efficient survey of the area.